LETTER

Polar Coding Aided by Adaptive Channel Equalization for Underwater Acoustic Communication

Feng LIU[†], Qianqian WU[†], Conggai LI[†a)], Fangjiong CHEN[††], *Nonmembers*, *and* Yanli XU[†], *Member*

SUMMARY To improve the performance of underwater acoustic communications, this letter proposes a polar coding scheme with adaptive channel equalization, which can reduce the amount of feedback information. Furthermore, a hybrid automatic repeat request (HARQ) mechanism is provided to mitigate the impact of estimation errors. Simulation results show that the proposed scheme outperforms the turbo equalization in bit error rate. Computational complexity analysis is also provided for comparison.

key words: *polar coding, adaptive equalization, feedback, HARQ, underwater acoustic communications*

1. Introduction

Underwater acoustic (UWA) communication technology plays an important role in many fields, such as the exploration of marine resources [1]. However, a reliable and efficient communication is still a great challenge due to the complexity of UWA channels in terms of amplitude, time, frequency and space. Channel coding technology can resist the effect of noise, and equalization can mitigate intersymbol interference (ISI). These two technologies are often used together to improve the quality of UWA communication.

Polar code is the first method that theoretically reaches the Shannon limitation, and has lower coding complexity than low-density parity-check (LDPC) and Turbo codes. Nevertheless, there are few works studying on polar codes for the UWA channels [2]–[4]. Monte Carlo [2], [3] and Bhattacharyya boundary [3], [4] approaches are often used to construct polar codes. However, the former is based on statistical performances, while the latter requires the feedback of channel gains and noise variance. Both are unsuitable for practical UWA channels.

Adaptive decision feedback equalization (DFE) can automatically track the change of channel characteristics and avoid the complex process of channel estimation and matrix inversion. It is suitable for UWA channels with long storage length and can effectively suppress the ISI. Combining adaptive DFE and turbo decoding is effective with the minimum symbol-error rate (MSER) criterion [5]. However, it is shown to be time-consuming [6], [7].

Manuscript received March 13, 2022.
Manuscript revised June 5, 2022.
Manuscript publicized July 1, 2022.

[†]The authors are with the College of Information Engineering, Shanghai Maritime University, Shanghai, China.
[††]The author is with the School of Electronics and Information Engineering, South China University of Technology, Guangzhou, China.
a) E-mail: cgli@shmtu.edu.cn

DOI: 10.1587/transfun.2022EAL2024

This letter proposes a polar coding scheme with less feedback and low complexity based on adaptive equalization for UWA communications. The equalized UWA channel is approximated as Gaussian, and its equivalent noise variance σ^2 is estimated and fed back to the transmitter for polar encoding. Moreover, to overcome the influence of estimation error of σ^2, we further provide a hybrid automatic repeat request (HARQ) mechanism. Finally, simulation results and complexity analysis are given to validate the performance.

2. System Model

The system model is shown in Fig. 1. At the transmitter side, binary information sequence firstly undergoes polar encoding, where the equivalent noise variance σ^2 of the UWA channel is fed back by the receiver after equalization. Then binary phase shift keying (BPSK) modulation transforms the encoded binary sequence into signals, which is then transmitted through the UWA channel. At the receiver side, the received signal in the k-th time slot can be expressed as

$$r_k = \sum_{i=0}^{M-1} h_i s_{k-i} + n_k \tag{1}$$

where s_k represents the modulated symbol, h_i denotes the channel impulse response (CIR), M is the maximum delay spread of the channel, and n_k represents the additive white Gaussian noise (AWGN) with zero mean and variance σ_0^2. The received signal is equalized to suppress the ISI. Here we use the adaptive DFE based on the MSER criterion [5]. Both the receiver and transmitter share the training data.

The output of the DFE in the k-th time slot and the update process of the equalizer coefficients are expressed as

$$y_k = \boldsymbol{f}_k^T \boldsymbol{r}_k + \boldsymbol{b}_k^T \hat{\boldsymbol{s}}_k \tag{2}$$

$$\boldsymbol{f}_k = \boldsymbol{f}_{k-1} - \frac{u_f I_k}{\boldsymbol{r}_k^T \boldsymbol{r}_k} \boldsymbol{r}_k \tag{3}$$

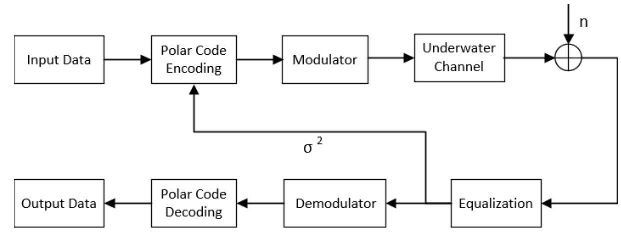

Fig. 1 Block diagram of the system model.

$$\boldsymbol{b}_k = \boldsymbol{b}_{k-1} - \frac{u_b I_k}{Q(\hat{\boldsymbol{s}}_k^T)Q(\hat{\boldsymbol{s}}_k)} Q(\hat{\boldsymbol{s}}_k) \tag{4}$$

where $I_k = \left(\tanh\left(\beta\left(\boldsymbol{f}_{k-1}^T \boldsymbol{r}_k + \boldsymbol{b}_{k-1}^T Q\left(\hat{\boldsymbol{s}}_k\right)\right)\right) - s_{k-D}\right)/2$, y_k is the equalizer output, $\boldsymbol{f}_k = [f_{k,0}, f_{k,1}, \cdots, f_{k,N_f-1}]^T$ is the feedforward filter with length of N_f, $\boldsymbol{b}_k = [b_{k,0}, b_{k,1}, \cdots, b_{k,N_b-1}]^T$ is the feedback filter with length of N_b, β is a predefined constant, $\hat{\boldsymbol{s}}_k = [\hat{s}_{k-D-1}, \hat{s}_{k-D-2}, \cdots, \hat{s}_{k-D-N_b}]$ is the N_b past detected symbols with delay D, u_f and u_b are the corresponding step sizes, and $Q(\cdot)$ denotes the symbol decision operation.

3. Proposed Scheme

3.1 Equivalent Noise Variance Estimation

The equalization output can be expressed as follows

$$\hat{s}_k = \lambda s_k + \hat{n}_k \tag{5}$$

where λ is the bias introduced by the equalizer, $\hat{n}_k$ is the residual interference after equalization which can be modeled as a Gaussian random variable with zero mean. After further eliminating the equalizer bias, y_k can be regarded as the result of signal s_k passing through the Gaussian channel

$$y_k = \frac{\hat{s}_k}{\lambda} = s_k + \frac{\hat{n}_k}{\lambda} \tag{6}$$

Equalizer bias λ can be calculated according to the average value of the equalizer output in time. If the received training data length is T, the calculation of λ can be expressed as

$$\lambda = \frac{\sum_{k=1}^{T} \hat{s}_k / s_k}{T} \tag{7}$$

Similarly, the noise variance σ^2 of the equivalent Gaussian channel can be given by:

$$\sigma^2 = \frac{\sum_{k=1}^{T} |\hat{s}_k - \lambda s_k|^2}{T\lambda^2} \tag{8}$$

3.2 Polar Encoding

With σ^2, we can use the Gaussian approximation (GA) method for polar encoding. Denote the number of subchannels as N. The mean log-likelihood ratio $m_N^{(n)}$ of the n-th sub-channel $W_N^{(n)}$ can be calculated by [8] as $\forall n = 1, \cdots, N$

$$m_N^{(n)} = \begin{cases} 2m_{N/2}^{(n/2)}, & \text{even } n \\ \phi^{-1}\left(1 - \left(1 - \phi\left(m_{N/2}^{((n+1)/2)}\right)\right)^2\right), & \text{odd } n \end{cases} \tag{9}$$
$$m_1^{(1)} = \frac{2}{\sigma^2}$$

where the function $\phi(x)$ is defined as

$$\phi(x) = \begin{cases} \exp\left(-0.4527x^{0.86} + 0.0218\right), & 0 < x < 10 \\ \sqrt{\frac{\pi}{x}} \exp\left(-\frac{x}{4}\right)\left(1 - \frac{10}{7x}\right), & x \geq 10 \end{cases} \tag{10}$$

After $m_N^{(n)}$ is obtained, the decoding error probability $P(W_N^{(n)})$ of each sub-channel can be calculated as follows

$$P(W_N^{(n)}) = \int_{-\infty}^{0} \frac{1}{2\sqrt{\pi m_N^{(n)}}} \cdot \exp\left(\frac{-\left(x - m_N^{(n)}\right)^2}{4m_N^{(n)}}\right) dx \tag{11}$$

According to the sub-channel reliability ranking, we take the K sub-channels with the highest reliability as the information bit indexes of the channel, and the remaining $N-K$ sub-channels as the frozen bit indexes of the channel. After mixing the information bits and the frozen bits according to the index position, the sequence to be encoded $\boldsymbol{u}_1^N$ is obtained. The encoding process can be expressed as [9]

$$\boldsymbol{x}_1^N = \boldsymbol{u}_1^N \boldsymbol{G}_N \tag{12}$$

where $\boldsymbol{G}_N$ is the generator matrix, $\boldsymbol{u}_1^N$ and $\boldsymbol{x}_1^N$ are the sequence before and after encoding, respectively. The generator matrix can be defined as $\boldsymbol{G}_N = \boldsymbol{B}_N \boldsymbol{F}^{\otimes s}$, where $s = \log(N)$, $\boldsymbol{F} = \begin{bmatrix} 1 & 0 \\ 1 & 1 \end{bmatrix}$, $\boldsymbol{B}_N$ is bit-inverse matrix which can be obtained according to $P(W_N^{(n)})$, and $\boldsymbol{F}^{\otimes s}$ is the operation of the Kronecker product of s times for the matrix $\boldsymbol{F}$.

3.3 Polar Decoding and HARQ Mechanism

Here we choose the cyclic redundancy check (CRC)-aided successive cancellation list (CA-SCL) decoding algorithm for polar decoding [10]. Firstly, we perform CRC on the K_1-bit information bits to obtain the K_2-bit CRC sequence. Then the $K = K_1 + K_2$ bit sequence is treated as the input of the polar encoding. The decoding process sets the search width L and saves the L decoding paths according to the probability values from large to small. With path selection, CRC is performed on the saved decoding paths in turn. If there is a path that passes the CRC, it will be the decoding result, and the decoding process ends. If all candidate decoding paths fail the CRC, the candidate path with the largest probability value is taken as the final decoding result.

Furthermore, we introduce a HARQ mechanism shown in Fig. 2 to mitigate the impact of equivalent noise estimation error (i.e., σ^2) and improve the bit error rate (BER) performance. If the decoding result passes the CRC, the receiver

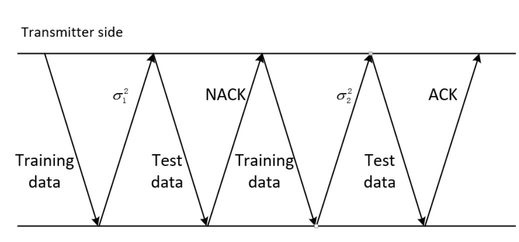

Fig. 2 The proposed HARQ mechanism.

will send the acknowledgement (ACK) to the transmitter, which ends the transmission of this frame. If no decoding path passes the CRC, a negative ACK (NACK) frame will be fed back. Then the transmitter sends the training data again to update the σ^2 feedback. The originally transmitted data will be re-encoded and transmitted until the CRC succeeds or the maximum number of retransmissions is reached [11].

The update process of σ^2 at the jth feedback can be expressed as

$$\sigma^2 = \sigma_j^2 \tag{13}$$

4. Simulation and Analysis

In this section, we compare the performance of the proposed scheme and the turbo equalization [5] through simulations, which use the same CIR as in [5]. We assume that the channel is time-invariant during a complete training and testing period. In the training period, the transmitted symbols are known to the receiver as training sequence and the training data obey an independent and identical distribution. Training data length T will affect the convergence of the equalizer coefficients and the accuracy of σ^2. Therefore, we use training data with different lengths for comparison, and fix the test frame length as 512 bits (496 information bits + 16 CRC bits). The transmitter performs polar encoding at a coding rate of 1/2. For comparison, the turbo equalization uses the same amount of training data to update the equalizer coefficients, and then uses a 1/2-rate recursive systematic convolution (RSC) encoder with the generator polynomial $[G_1, G_2] = [5, 7]$ for one frame test data to perform convolutional encoding. The convolutional encoded sequence is transmitted through the pseudo-random interleaver.

Table 1 shows the control variables of the equalizer, where N_f, N_b are the numbers of taps for the feedforward and the feedback filters, respectively. It should be emphasized that the turbo equalization updates its coefficients with a smaller step size in the test period than that in the training period to avoid error propagation. In contrast, the proposed polar scheme needs to keep the equalizer coefficients unchanged to avoid inaccurate calculations of σ^2.

4.1 FER and BER Performance

In the simulation, we set two training data lengths, 512 bits and 1024 bits. As the length of training data increases, the performance of the equalizer will be improved. Figure 3 and Fig. 5 show that when the equalization effect is good, the polar codes scheme proposed in this paper outperforms the turbo equalization with 5 iterations by at least 1 dB in terms of frame error rate (FER). But in Fig. 4 and Fig. 6, the BER performance of the proposed scheme is not as good as the turbo equalization with 5 iterations. This is due to the characteristic of sequential decoding of polar codes. When decoding errors occur, a large number of incorrectly decoded bits will be caused. Similar phenomenon has been observed in [12] for radio communications.

Figures 7 and 8 respectively show the FER and BER results by using HARQ mechanism (the maximum number of retransmissions is set to 1) when the training data length is 1024 bits. It can be seen that the FER of the polar coding scheme converges rapidly when SNR = 6, which makes the BER of the polar codes quickly drop to zero. In contrast, the improvement effect on the turbo equalization is relatively small.

4.2 Computational Complexity

Table 2 gives a complexity comparison with related de-

Table 1 The control parameters of coding mode.

Scheme	Convolutional codes		Polar codes	
Filter	Feedforward	Feedback	Feedforward	Feedback
Train mode	$u_f = 0.15$	$u_b = 0.25$	$u_f = 0.15$	$u_b = 0.25$
Test mode	$u_f = 0.01$	$u_b = 0.01$	$u_f = 0$	$u_b = 0$
Number of taps	$N_f = 120$	$N_b = 80$	$N_f = 120$	$N_b = 80$

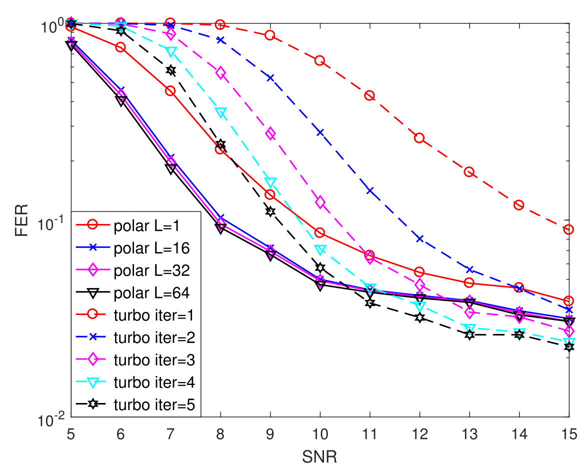

Fig. 3 Comparison of FER performance of polar codes and turbo equalization with $T = 512$.

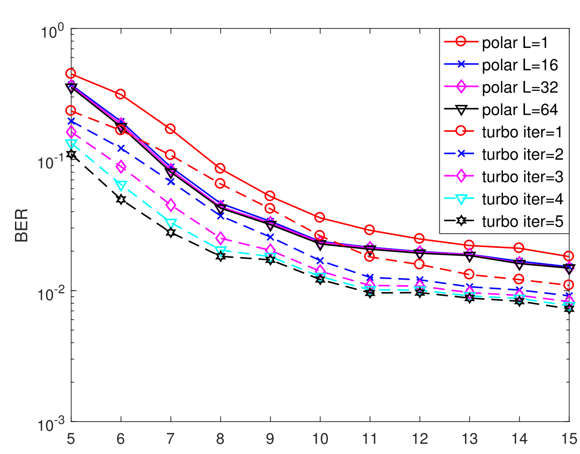

Fig. 4 Comparison of BER performance of polar codes and turbo equalization with $T = 512$.

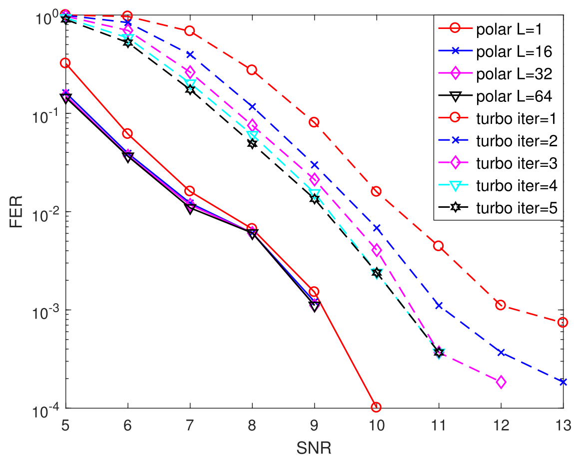

Fig. 5 Comparison of FER performance of polar codes and turbo equalization with $T = 1024$.

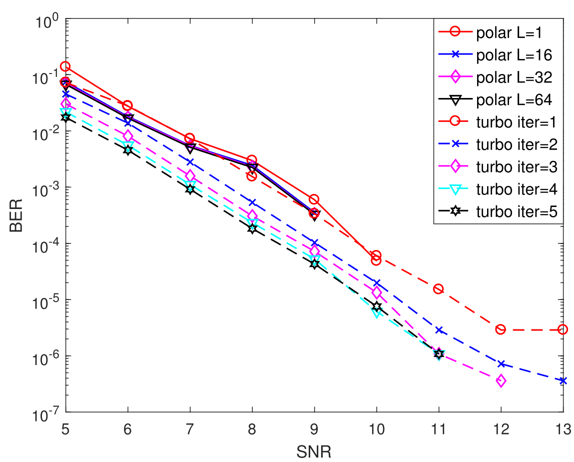

Fig. 6 Comparison of BER performance of polar codes and turbo equalization with $T = 1024$.

coders in [13], [14], where N, K, L denote the code length, the length of the information to be encoded and the search width of the decoding algorithm, respectively. Also, we have $S = 2^m$, where m is the number of encoding registers. And $I_{\max}$ represents the maximum number of iterations during decoding. The complexity of the decoder depends on the related variables. It is not obvious which is lower. For a typical configuration, the complexity comparison is shown in Table 3, from which we can see that the decoding complexity of the polar code scheme is lower than that of turbo decoding. In addition, the complexities of polar encoder and GA construction are $O(N\log(N))$ and $O(N)$, respectively.

5. Conclusion

This paper proposed an equalization assisted polar coding scheme. With the proposed scheme, constructing polar codes suitable for UWA channels only needs to feed back the equivalent noise variance at the equalization output, which greatly reduces the feedback requirement. With the given HARQ mechanism, the impact of estimation errors can be further mitigated. Simulation results show that compared with the turbo equalization, the proposed scheme has better BER performance and lower decoding computational complexity for the given configuration.

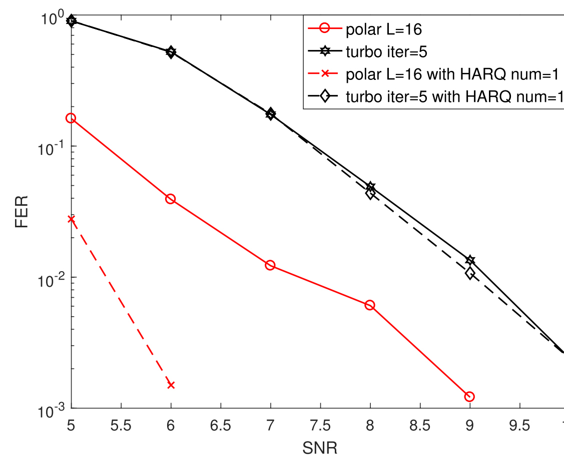

Fig. 7 FER comparison with/without HARQ mechanism with $T = 1024$.

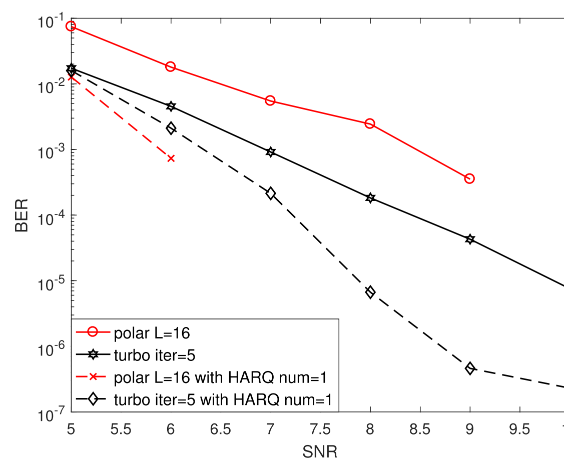

Fig. 8 BER comparison with/without HARQ mechanism with $T = 1024$.

Table 2 Complexity comparison of related receivers.

Channel decoder	Additions	MAX process / Comparison
Polar (SCL)	$LN\log(N)+LN+2LK\log(2L)$	NA
Turbo (Max-log-MAP)	$16NSI_{\max}$	$8NSI_{\max}$

Table 3 Specified decoding complexity in simulation.

Channel decoder	N	K	L	m	$I_{\max}$	Complexity
Polar (SCL)	1024	512	16	—	—	245760
Turbo (Max-log-MAP)	1024	512	—	3	5	655680

Acknowledgments

This research was funded by the Innovation Program of Shanghai Municipal Education Commission of China (2021-

01-07-00-10-E00121), the National Natural Science Foundation of China (U1701265), and the Natural Science Foundation of Shanghai (20ZR1423200).

References

[1] T. Qiu, Z. Zhao, T. Zhang, C. Chen, and C.L.P. Chen, "Underwater internet of things in smart ocean: System architecture and open issues," IEEE Trans. Ind. Inf., vol.16, no.7, pp.4297–4307, 2020.

[2] G. Qiao, S. Xing, and F. Zhou, "A multi-user detection scheme based on polar code construction in downlink underwater acoustic OFDM communication system," IEEE Access, vol.7, pp.65973–65981, 2019.

[3] Y. Zhai, J. Li, and H. Feng, "Research on polar coding application for underwater acoustic OFDM communication system," 2020 IEEE 6th International Conference on Computer and Communications (ICCC), pp.322–328, 2020.

[4] L. Xing, Z. Li, Z. Zhang, and C. Zhao, "Research on the application of polar codes in underwater acoustic communication," 2021 7th International Conference on Computer and Communications (ICCC), pp.115–119, 2021.

[5] F. Chen, S. Lin, B. Zheng, Q. Li, M. Wen, Y. Liu, and F. Ji, Minimum symbol-error rate based adaptive decision feedback equalizer in underwater acoustic channels," IEEE Access, vol.5, pp.25147–25157, 2017.

[6] L. Xu, X. Zhong, H. Yu, F. Chen, F. Ji, and S. Yan, Spatial and time-reversal diversity aided least-symbol-error-rate turbo receiver for underwater acoustic communications," IEEE Access, vol.6, pp.9049–9058, 2018.

[7] A.-M. Cuc, F.L. Morgoş, C. Grava, S. Curilă, and T.A. Burcă, "Performances comparison between turbo codes and polar codes," 2021 16th International Conference on Engineering of Modern Electric Systems (EMES), pp.1–4, 2021.

[8] P. Trifonov, "Efficient design and decoding of polar codes," IEEE Trans. Commun., vol.60, no.11, pp.3221–3227, 2012.

[9] E. Arikan, "Channel polarization: A method for constructing capacity-achieving codes for symmetric binary-input memoryless channels," IEEE Trans. Inf. Theory, vol.55, no.7, pp.3051–3073, 2009.

[10] K. Niu and K. Chen, CRC-aided decoding of polar codes," IEEE Commun. Lett., vol.16, no.10, pp.1668–1671, 2012.

[11] T. Yu and W. Nie, "Research on polarization code encoding and decoding algorithm based on HARQ technology," 2019 IEEE 3rd Information Technology, Networking, Electronic and Automation Control Conference (ITNEC), pp.2517–2521, 2019.

[12] Z. He, X. Li, S. Wang, and Y. Qi, "A noise-assisted polar code attempt decoding algorithm," 2021 IEEE 13th International Conference on Computer Research and Development (ICCRD), pp.73–77, 2021.

[13] Z.R.M. Hajiyat, A. Sali, M. Mokhtar, and F. Hashim, "Channel coding scheme for 5G mobile communication system for short length message transmission," Wireless Personal Communications, vol.106, no.2, pp.377–400, 2019.

[14] NTT, Evaluation of polar codes for eMBB, 2016.